Environmental Technology & Innovation 23 (2021) 101615

Contents lists available at ScienceDirect

Environmental Technology & Innovation

journal homepage: www.elsevier.com/locate/eti

The adsorption of U(VI) on magnetite, ferrihydrite and goethite

Yun Wang [a,b], Jingjing Wang [a,b], Ping Li [a,b,*], Haibo Qin [c,**], Jianjun Liang [a,b], Qiaohui Fan [a,b]

[a] Northwest Institute of Eco-Environment and Resources, Chinese Academy of Sciences, Lanzhou 730000, China
[b] Key Laboratory of Petroleum Resources, Gansu Province, Lanzhou 730000, China
[c] State Key Laboratory of Environmental Geochemistry, Institute of Geochemistry, Chinese Academy of Sciences, Guiyang 550081, China

ARTICLE INFO

Article history:
Received 13 April 2021
Received in revised form 5 May 2021
Accepted 10 May 2021
Available online 12 May 2021

Keywords:
Uranium
Iron oxides
Adsorption
Anaerobic condition
Reduction

ABSTRACT

During the long-term disposal of radioactive waste, ferrous waste containers and building materials are tending to corrode to produce a large number of iron oxides. The formed iron oxides would bring significant effects on the diffusion and migration of radionuclides through adsorption and reduction. This study aimed to evaluate the interaction of U(VI) on iron oxides under anaerobic conditions, where goethite, magnetite, and ferrihydrite were used as adsorbents. The results showed that the adsorption of U(VI) on iron oxides was chemical adsorption, and the adsorption capacity of U(VI) on ferrihydrite was much higher than that on goethite and magnetite. Humic acid (HA) promoted the adsorption of U(VI) on iron oxides under acidic conditions, while U(VI) adsorption was inhibited by HA in the neutral to alkaline conditions. The adsorption of U(VI) on iron oxides was an endothermic process, and higher temperature was beneficial for the adsorption. Surface complexation modeling (SCM) fitting revealed that monodentate inner complexes of $\equiv FeOUO_2^+$ and $\equiv FeOUO_2(OH)^0$ were mainly formed on the surface of iron oxides. Finally, the reduction of U(VI) to U(IV) on magnetite under anaerobic condition was confirmed by X-ray photoelectron spectroscopy (XPS) and Mössbauer spectroscopy.

1. Introduction

It was predicted by the International Atomic Energy Agency that global nuclear power production may increase by up to 56% over the period 2015–2030 (Tsouris, 2017). As the fast development of nuclear energy, a large amount of radioactive wastes will be produced, bringing safety threats to the environment and human health (Janaun and Ellis, 2011). The safe disposal of these wastes therefore has attracted worldwide attentions. To date, the deep geological disposal has been recognized as the most effective and feasible method for treating high-level radioactive wastes.

In the disposal repository, multiple barriers are designed for avoiding the release of radionuclides, where carbon steel containers are applied to pack the radioactive wastes (Sellin and Leupin, 2013). However, during the long-term disposal of wastes, the container may fail due to the corrosion caused by the groundwater penetrated into the repository (Smailos

* Corresponding author at: Northwest Institute of Eco-Environment and Resources, Chinese Academy of Sciences, Lanzhou 730000, China.
** Corresponding author.
E-mail addresses: liping@lzb.ac.cn (P. Li), qinhaibo@eps.s.u-tokyo.ac.jp (H. Qin).

https://doi.org/10.1016/j.eti.2021.101615
2352-1864/

et al., 1991). In this scenario, the corrosion products of the iron containers should become a pivotal barrier to control and retard the migration of radionuclides (Grambow et al., 1996). Moreover, the abundant iron building materials and devices in repository will also be subjected to corrosion, forming huge amount of iron oxides (Grambow et al., 1996). Generally, iron oxides can affect the diffusion and migration of radionuclides in two ways: (1) reducing environment can be formed after the corrosion of iron, causing the reduction of multivalent radionuclides; (2) iron oxides have a large specific surface area and strong adsorption capacity, which can block the migration of radionuclides. Therefore, the adsorption of radionuclides on iron oxides is important for evaluating the environment safety of radioactive elements.

Uranium is one of the most extensive and important elements in the nuclear industry, and about 96% of the spent nuclear fuel is UO_2 at the end of the fuel's useful life in the reactor (Ewing, 2015). As a result, the physicochemical and environmental behaviors of uranium have received extensive attention (Li et al., 2019; Wang et al., 2020). As well known, under natural conditions, uranium typically occurs in its hexavalent valence state in the form of soluble UO_2^{2+}, which is easy to migrate. Therefore, the immobilization of U(VI) at solid/water interface closely relates to its environmental fate. To date, the adsorption of U(VI) on natural and artificial substrates has been widely estimated using batch and column approaches (Dong et al., 2020; Liu et al., 2018; Mei et al., 2020; Payne et al., 1996; Qian et al., 2015; Wang et al., 2019). However, most of the previous works focused on the environmental behavior of U(VI) in open systems. It is generally believed that the dissolved oxygen concentration in the underground disposal environment is low owing to the diffusion of dissolved oxygen into the surrounding geological bodies, and the oxidation of certain components in the minerals such as bentonite (Shoesmith, 2006), and the oxygen consumption during the corrosion of the metal disposal tank (El Hajj et al., 2013). It is expected that the discrepancy in the conditions including atmosphere and redox potential should bring difference to the environmental behavior of U(VI). Therefore, the study of the interaction between U(VI) and iron oxides under anaerobic conditions has more practical significance (Dodge et al., 2002; Duro et al., 2008; Grambow et al., 1996). Moreover, iron-containing packaging containers can typically form various types of iron oxides, including Fe_3O_4, α-FeOOH, γ-FeOOH, $Fe_2O_3{\bullet}H_2O$, and γ-Fe_2O_3 (Dodge et al., 2002). Due to the difference of structure and surface properties, the interaction mechanisms between different iron oxides and U(VI) are expected to be different. Therefore, the comparison of the adsorption affinity of these minerals for U(VI) is important for better estimating the adsorption of U(VI) on the corrosion products.

In this paper, three typical iron oxides (α-FeOOH, Fe_3O_4, ferrihydrite) were selected to study the adsorption of U(VI) under anaerobic conditions. The effects of pH, organic matters, temperature and other environmental factors on the adsorption of U(VI) on three iron oxides were investigated. Finally, the interaction mechanism between U(VI) and iron oxides under anaerobic conditions was also discussed.

2. Materials and methods

2.1. Chemicals and materials

All the chemicals used in this experiment are of analytical purity without further treatment. Uranyl solution is obtained by dissolving $UO_2(NO_3)_2{\bullet}6H_2O$ in Milli-Q water, and then stored at pH ~3.0. Humic acid (HA) was extracted from Gannan soil, and has been characterized in our previous work (Fan et al., 2008).

2.2. Characterization

X-ray photoelectron spectroscopy (XPS) analysis of all samples were conducted on the ESCALAB250xi spectrometer (Thermo Fisher Scientific). The binding energies were referenced by the C 1s at 284.6 eV. The Mössbauer spectra were obtained at room temperature (25 °C) using WissEl MB-500 Mössbauer with a ^{57}Co (Rh) source.

2.3. Batch experiments

All the experiments were conducted in N_2 atmosphere. Adsorption kinetics were conducted over a time range of 0 to 4320 min in 250 mL glass bottles containing 0.6 g L^{-1} suspension of iron oxides, 1.0×10^{-4} mol L^{-1} U(VI), 0.01 mol L^{-1} NaCl at pH ~4.8. At desired time, the above suspension was filtered with 0.22 μm membrane. The concentration of U(VI) in the supernatant was measured by UV–Vis spectrophotometer at 652 nm using Arsenazo III as dye.

The adsorption edge was carried out in 6 mL suspension containing 0.6 g L^{-1} iron oxides, 0.01 mol L^{-1} NaCl solution, and 1.0×10^{-4} mol L^{-1} U(VI) solution over pH range from 3.0 to 7.0, and the following steps were in accordance with the adsorption kinetics.

For the competition adsorption of iron oxides for U(VI), experiments were conducted using semipermeable bags to separate three kinds of iron oxides in a U(VI)-containing system. Briefly, 0.1 g goethite, magnetite, and ferrihydrite were put into three semipermeable bags, respectively, and were immersed into 500 mL of 1.0×10^{-5} mol L^{-1} U(VI) solution. The pH of U(VI) solution was adjusted to 5.0 and 6.5 with 0.1 mol L^{-1} HCl and/or NaOH solution. After reaction for 24 h, U(VI) adsorbed on iron oxides was desorbed with 0.1 mol L^{-1} Na_2CO_3 solution for 12 h. Finally, the concentration of U(VI) was measured by above-mentioned method.

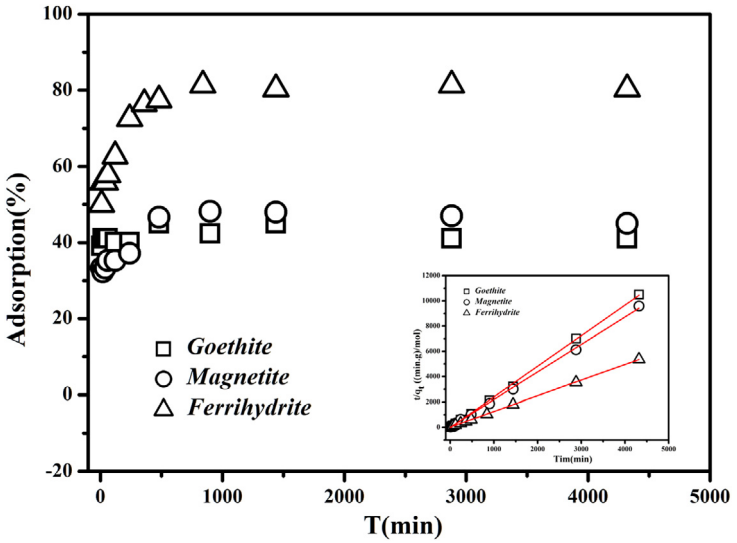

Fig. 1. Effect of time on the adsorption of U(VI) to iron oxides, and the application of the pseudo-second-order model to the adsorption of U(VI) (insert). m/V = 0.6 g L^{-1}, [UO_2^{2+}] = 1.0 × 10^{-5} mol L^{-1}, [NaCl] = 0.01 mol L^{-1}, pH = 4.8 ± 0.1, T = 25 ± 1 °C.

Adsorption isotherms at different temperatures (25, 45, 60 °C) were carried out over the concentration of U(VI) from 2.5 mg L^{-1} to 250 mg L^{-1} in 10 mL polyethylene tubes containing 0.6 g L^{-1} suspension of iron oxides and 0.01 mol L^{-1} NaCl at pH ~4.8. The following steps were the same as the above experiments. The adsorption percentages were calculated from the equation:

$$\text{Adsorption}\ (\%) = \frac{C_0 - C_e}{C_0} \times 100\% \tag{1}$$

where C_0 (mol L^{-1}) and C_e (mol L^{-1}) are the initial and final concentrations of U(VI) in the solution.

3. Result and discussion

3.1. Sorption kinetics

U(VI) adsorption to iron oxides as a function of reaction time is depicted in Fig. 1. As can be seen from Fig. 1, the adsorption of U(VI) on goethite achieved equilibrium within 10 min. In contrast, the adsorption of U(VI) on magnetite and ferrihydrite achieved equilibrium at 480 and 840 min, respectively. It was obvious that the adsorption amount of U(VI) on ferrihydrite (80.38%) is higher than that on goethite (41.13%) and magnetite (45.05%). In order to study the adsorption kinetics of U(VI) on iron oxides, the pseudo-first-order model and the pseudo-second-order kinetic equation were applied to fit the adsorption kinetics. The linear form of the pseudo-first-order (Eq. (2)) (Ho and McKay, 2000) and pseudo-second-order (Eq. (3)) (Fan et al., 2012; Gao et al., 2010) kinetic models are presented as follows:

$$\ln(q_e - q_t) = \ln q_e - k_1 t \tag{2}$$

$$\frac{t}{q_t} = \frac{1}{k_2} q_e + \frac{t}{q_e} \tag{3}$$

where q_e (mol g^{-1}) is the equilibrium adsorption amount, and q_t is the adsorption amount of U(VI) at time t. The parameter k_1 (min^{-1}) and k_2 (g (mol min)$^{-1}$) represent the rate constants of the pseudo-first-order and pseudo-second-order kinetic model, respectively. As can be seen from Table S1 (in the Supporting Information), the q_e obtained from pseudo-second-order kinetic equation are closer to those obtained from experiments, and the correlation coefficient R^2 values are closer to one than that obtained from pseudo-first-order model. This indicated that the adsorption of U(VI) on three iron oxides can be described well by the pseudo-second-order kinetic model, and the adsorption kinetics of U(VI) was mainly controlled by the initial concentration of U(VI) and the amount of iron oxides in the system (Li et al., 2015). In addition, this kinetic process could also prove that the adsorption reaction may be predominantly chemisorption (Ho and McKay, 2000).

3.2. Effect of pH

pH is one of the most important factors affecting the adsorption process by controlling the surface properties of adsorbents as well as the chemical species of metal ions. The adsorption of U(VI) on iron oxides as a function of pH

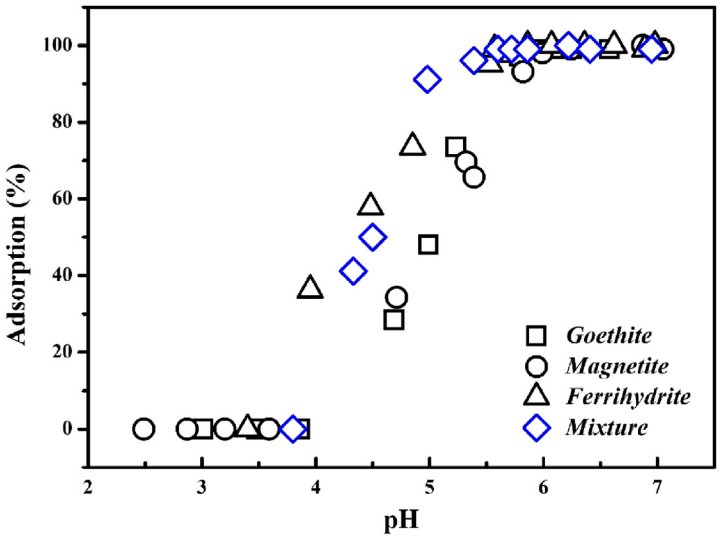

Fig. 2. Effect of pH on U(VI) adsorption onto iron oxides. m/V = 0.6 g L^{-1}, [UO_2^{2+}] = 1.0 × 10^{-5} mol L^{-1}, [NaCl] = 0.01 mol L^{-1}. Mixture was prepared by mixing the three iron oxides in the same proportion.

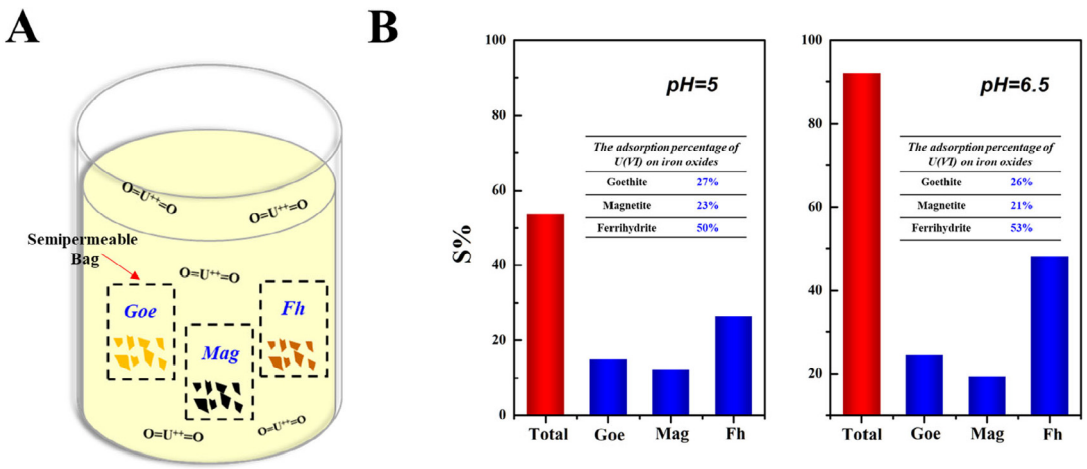

Fig. 3. Competitive adsorption of iron oxides for U(VI). m/V = 0.6 g L^{-1}, [UO_2^{2+}] = 1.0 × 10^{-5} mol L^{-1}, [NaCl] = 0.01 mol L^{-1}, T = 25 ± 1 °C. Installation diagram of competitive adsorption of U(VI) on three iron oxides (A), and the results of competitive adsorption of U(VI) by iron oxides at pH 5.0 and 6.5 (B).

was studied at varying pH values (Fig. 2). It can be seen that pH played an important role in the adsorption of U(VI) on iron oxides. The adsorption of U(VI) increased gradually when the pH increased from 3.0 to 6.0. This might be due to the increasing deprotonated adsorption sites with the increase of pH value (Hattori et al., 2009; Rossberg et al., 2009; Sylwester et al., 2000). At the meantime, U(VI) predominantly occurred in the form of UO_2^{2+} and UO_2OH^+ over this pH range (Fig. S1 in the Supporting Information), which was more easily adsorbed onto the negatively charged surface of adsorbents. At pH ~6.0, almost complete removal of U(VI) was achieved. It was obvious that the adsorption of U(VI) on magnetite and goethite was very closed, and ferrihydrite showed the highest affinity for U(VI) over the whole pH range, which may be due to its relatively larger specific surface area (340 m^2 g^{-1}) than goethite (86 m^2 g^{-1}) and magnetite (106 m^2 g^{-1}) (Eggleton and Fitzpatrick, 1988).

3.3. Competition adsorption for U(VI)

The iron oxides found on corroding steel surfaces typically include ferrihydrite, goethite, magnetite, hematite, lepidocrocite and maghemite (Dodge et al., 2002). Owing to the discrepancy in the reaction affinity of these iron oxides for U(VI), it is important to evaluate the adsorption of U(VI) on the mixture of iron oxides as well as each individual iron

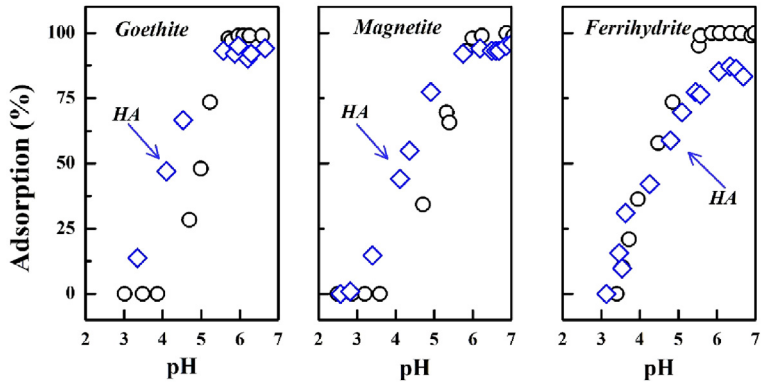

Fig. 4. Effect of HA on U(VI) adsorption onto goethite, magnetite, ferrihydrite. $m/V = 0.6$ g L^{-1}, $[UO_2^{2+}] = 1.0 \times 10^{-5}$ mol L^{-1}, [HA] = 25 mg L^{-1}, [NaCl] = 0.01 mol L^{-1}, T = 25 ± 1 °C.

oxide. The kinetic study in Fig. 2 shows that the adsorption of U(VI) on ferrihydrite was much stronger than goethite and magnetite. When mixing the three iron oxides in the same proportion to adsorb U(VI), the adsorption of U(VI) on the mixture was greater than goethite and magnetite, but slightly weaker than ferrihydrite (Fig. 2). To further study the competition adsorption of U(VI) on each iron oxide of the mixture, iron oxides were enclosed in the semipermeable bags, and were immersed in solution containing 1.0×10^{-5} mol L^{-1} U(VI) (Fig. 3A). The results show that the removal percentage of U(VI) by the iron oxides reached 53.66%, 92.11% at pH 5.0 and 6.5, respectively (Fig. 3B). The measured adsorption percentage of U(VI) on three iron oxides at pH 5.0 was 27% on goethite, 23% on magnetite, and 50% on ferrihydrite. At pH 6.5, 26%, 21% and 53% of U(VI) was adsorbed by goethite, magnetite, and ferrihydrite, respectively. The results indicated that the adsorption of U(VI) on the three iron oxides follows the sequence of ferrihydrite > goethite ≈ magnetite. The highest adsorption affinity of ferrihydrite for U(VI) should be mainly owing to the largest specific surface area, resulting sufficient reaction sites for U(VI). However, it should be noted that although ferrihydrite showed the highest adsorption ability for U(VI), considerable U(VI) could be adsorbed by the other iron oxides. This means each kind of iron oxide could play an important role in the immobilization of U(VI) and should not be neglected.

3.4. Effect of HA

As an important ligand, HA is a ubiquitous organic substance in the nature, which is typically of significant importance to the environmental fate of metal ions (Li et al., 2015). The effect of HA on the adsorption of U(VI) on iron oxides was studied under different pH values. As shown in Fig. 4, the adsorption of U(VI) on goethite and magnetite could be promoted by HA at pH < 6.0, while it was inhibited at higher pH. At acidic conditions, the surface of goethite and magnetite was negatively charged, which was easy to attract negatively charged HA molecules. The strong interactions between U(VI) and the functional groups in HA would subsequently enhance the uptake of U(VI). In contrast, at higher pH of > 6.0, the surface of goethite and magnetite turned to be negatively charged, being hard to adsorb HA. The dissolved HA molecules in solution would form soluble complexes with U(VI), making U(VI) hard to be adsorbed by iron oxides (Schmeide et al., 2000). It is noticed that, different from goethite and magnetite, HA was observed to slightly facilitated the adsorption of U(VI) on ferrihydrite at pH < 4.0. At pH > 4.0, U(VI) adsorption onto ferrihydrite was inhibited in the presence of HA. This discrepancy might be caused by the difference in the adsorption of HA on these iron oxides. It is considered that the adsorption of HA on ferrihydrite was weaker than that on goethite and magnetite, and more HA molecules were dissolved into solution to form soluble U(VI)-HA complexes. Therefore, the presence of HA would bring stronger inhibition on U(VI) adsorption on ferrihydrite than goethite and magnetite.

3.5. Effect of temperature and thermodynamic estimation

Temperature is one of the most important factors determining the adsorption behavior of radionuclides (Wang et al., 2019). Fig. 5 shows the adsorption isotherms of U(VI) on iron oxides at different temperatures (25, 45, 60 °C). The amount of U(VI) adsorbed by three iron oxides increased with the increase of temperature, which indicated that the adsorption of U(VI) by iron oxides was endothermic reaction. In order to further explore the adsorption mechanism of U(VI) on iron oxides, the adsorption isotherms were fitted by Langmuir and Freundlich thermodynamic models. The linear form of the Langmuir isotherm (Eq. (4)) (Langmuir, 1918) and Freundlich model (Eq. (5)) (Freundlich, 1906) can be respectively represented as follows:

$$q_e = \frac{K_L q_{max} C_e}{1 + K_L C_e} \tag{4}$$

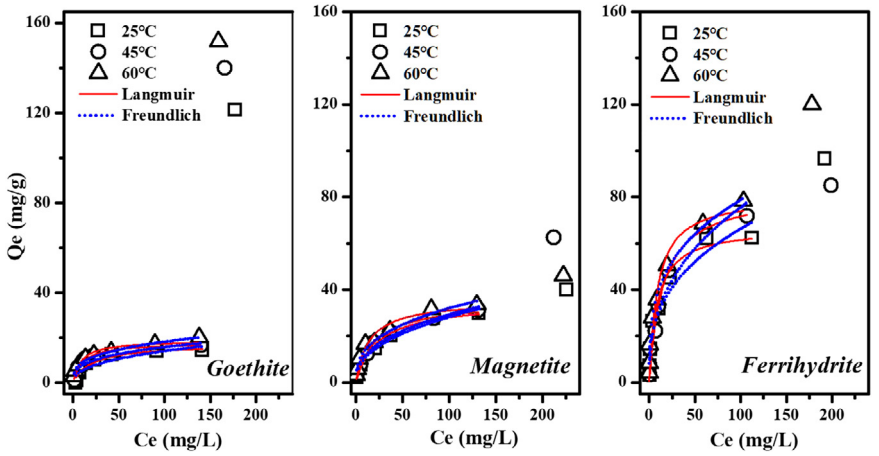

Fig. 5. Effect of temperature on the adsorption of U(VI) onto goethite, magnetite, ferrihydrite. m/V = 0.6 g L^{-1}, pH = 4.8 ± 0.1, [UO_2^{2+}] = 1.0 × 10^{-5} mol L^{-1}, [NaCl] = 0.01 mol L^{-1}.

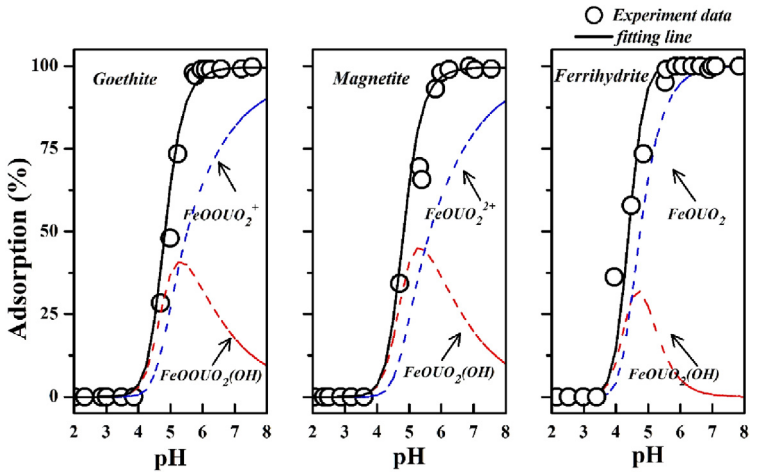

Fig. 6. Modeling of the adsorption species of U(VI) on goethite, magnetite, ferrihydrite as a function of pH.

$$q_e = K_F C_e^n \tag{5}$$

where C_e (mol L^{-1}) is the equilibrium concentration of U(VI) remaining in the solution; q_e (mol g^{-1}) means the amount of U(VI) adsorbed on per unit weight of iron oxides after equilibrium; q_{max} (mol g^{-1}) stands for the maximum adsorption capacity; K_L (L mol^{-1}) is the Langmuir constant; K_F (mol^{1-n} L^n g^{-1}) and n are the Freundlich constants. The thermodynamic parameters of Langmuir and Freundlich models are shown in Table S2. It shows that Langmuir model can fit the adsorption process of U(VI) on three iron oxides well, and the correlation coefficients R^2 are closer to 1.0 comparing with those fitted with Freundlich model. At 60 °C, the calculated adsorption capacity of goethite, magnetite and ferrihydrite for U(VI) were 19.1, 35.4 and 80.7 mg g^{-1}, respectively, which were very close to the experimental data (20.1, 33.5 and 78.3 mg g^{-1}). These results suggested that the Langmuir model fitted the experimental data well, indicating that the adsorption of U(VI) on three kinds of iron oxides was through monolayer adsorption or the adsorption occurred at a fixed number of localized sites. It was necessary to note that the adsorption of U(VI) on three iron oxides increased sharply at high U(VI) concentration, which was considered to be caused by the formation of precipitates on the surface (Li et al., 2014).

3.6. Modeling

In order to investigate the reactions between U(VI) and the iron oxides under anaerobic conditions, surface coordination model (SCM) was used to fit the adsorption data of U(VI) on iron oxides. The software used for fitting is Visual MINTEQ 3.0 code, assuming that the model is a diffusion layer model (2pK-DLM). 2pK-DLM model considers that charged mineral surface attracts ions from adjacent liquid phases and forms a double layer with charges on mineral surface. According to

Table 1
Modeling parameters for U(VI) adsorption on iron oxides.

Iron oxides	Reactions	logk
Goethite	$\equiv FeOH + UO_2^{2+} \leftrightarrow FeOUO^+ + H^+$	2.0
	$\equiv FeOH + UO_2^{2+} + H_2O \leftrightarrow FeOUO_2(OH)^0 + 2H^+$	−5.5
Magnetite	$\equiv FeOH + UO_2^{2+} \leftrightarrow FeOUO^+ + H^+$	2.0
	$\equiv FeOH + UO_2^{2+} + H_2O \leftrightarrow FeOUO_2(OH)^0 + 2H^+$	−5.5
Ferrihydrite	$\equiv FeOH + UO_2^{2+} \leftrightarrow FeOUO^+ + H^+$	3.0
	$\equiv FeOH + UO_2^{2+} + H_2O \leftrightarrow FeOUO_2(OH)^0 + 2H^+$	−2.0

Table 2
Mössbauer parameters of the iron components in the U(VI) adsorbed iron oxides at different conditions.

Samples	Iron species	Content (%)	IS (mm s^{-1})	QS (mm s^{-1})	HW (mm s^{-1})	B_{hf} (T)	Note
Raw (Li et al., 2017)	mag-Fe^{3+}	12.6	0.26 ± 0.01	0.00 ± 0.01	0.21 ± 0.01	49.71 ± 0.05	Fe_3O_4(A)
	mag- Fe^{2+} -Fe^{3+}	19.8	0.20 ± 0.01	−0.04 ± 0.03	0.40 ± 0.02	47.65 ± 0.22	Fe_3O_4(B)
	mag-Fe^{3+}	27.6	0.29 ± 0.01	−0.25 ± 0.01	0.38 ± 0.01	36.19 ± 0.04	α-FeOOH
	mag-Fe^{3+}	37.9	0.24 ± 0.02	−0.24 ± 0.03	0.94 ± 0.01	28.70 ± 0.18	Amorphous Fe_3O_4
	para-Fe^{3+}	2.2	0.45 ± 0.01	1.66 ± 0.01	0.18 ± 0.01	–	$Fe(OH)_3$
pH ~5.5	mag-Fe^{3+}	21.9	0.35 ± 0.01	0.02 ± 0.01	0.52 ± 0.02	49.30 ± 0.04	Fe_3O_4(A)
	mag- Fe^{2+} -Fe^{3+}	12.3	−0.12 ± 0.02	1.02 ± 0.04	0.77 ± 0.08	46.64 ± 0.15	Fe_3O_4(B)
	mag-Fe^{3+}	30.6	0.40 ± 0.01	−0.28 ± 0.01	0.78 ± 0.03	36.53 ± 0.05	α-FeOOH
	mag-Fe^{3+}	32.8	0.40 ± 0.02	0.16 ± 0.03	1.35 ± 0.05	27.92 ± 0.12	Amorphous Fe_3O_4
	para-Fe^{3+}	2.4	0.55 ± 0.01	1.71 ± 0.01	0.34 ± 0.02	–	$Fe(OH)_3$

the fitting results, the complexation species of U(VI) on all the three iron oxides can be depicted well by the following two reactions:

$$\equiv FeOH + UO_2^{2+} \leftrightarrow FeOUO_2^+ + H^+ \quad (6)$$

$$\equiv FeOH + UO_2^{2+} + H_2O \leftrightarrow FeOUO_2(OH)^0 + 2H^+ \quad (7)$$

The modeling results are shown in Fig. 6, and the related parameters are summarized in Table 1. The fitting results of SCM demonstrated that the main adsorption species of U(VI) on three iron oxides were $\equiv FeOUO_2^+$ at pH < 5.0, and $\equiv FeOUO^2(OH)^0$ above pH ~5.0 in the absence of CO_2. Li et al. (2014) found that the adsorption species of U(VI) on iron oxyhydroxides were composed of $\equiv FeOUO_2^+$ (pH < 4.5), $\equiv FeOUO_2(OH)^0$ and $\equiv FeOUO_2(CO_3)_2^{3-}$ (pH > 4.5) in the open environment. Considering the absence of CO_2 in the present study, the formed species of U(VI) on iron oxides surface are very similar.

3.7. Reduction of U(VI) by magnetite

X-ray photoelectron spectroscopy (XPS) and Mössbauer spectroscopy were applied to elucidate the adsorption and reduction of U(VI) on magnetite at molecule scale. As shown in Fig. 7A, U 4f peaks centered at 381.2 eV ($4f_{7/2}$) and 392.0 eV ($4f_{5/2}$) was observed after adsorption on magnetite for 24 h. However, after reaction for 30 days, obvious shift of U $4f_{7/2}$ peak from 381.2 eV to 381.0 eV could be observed. The fitting results confirmed that after reaction for 24 h, nearly no U(IV) could be found, which indicated that the reduction of U(VI) by magnetite was negligible in short reaction time. In contrast, after reaction for 30 days, the U $4f_{7/2}$ peak could be resolved into two peaks at 381.2 eV and 379.8 eV, corresponding to the U(VI) and U(IV) species, respectively. The fitting results clearly showed ~13% of U(VI) was reduced to U(IV) by magnetite after reacting for 30 days under anerobic conditions. It was reported that U(VI) could be reduced to U(IV) on the surface of magnetite (Dodge et al., 2002), in the form of amorphous UO_2 (Duro et al., 2008). El Aamrani et al. (2007) also found that the U(VI) adsorbed on the surface of magnetite occurred as the mixture of U(IV) and U(VI).

To further test the reduction of U(VI) by magnetite in the presence of other iron oxides, U(VI) was reacted with previously prepared iron oxyhydroxides, which was used as the analogue of iron corrosion products (Li et al., 2017). The adsorption and reduction of U(VI) can be deduced from the change of the structure information of Fe atoms obtained by Mössbauer spectroscopy. The fitting of the Mössbauer spectroscopy was shown in Fig. 7B, and the parameters were listed in Table 2. It was found that the hyperfine field (B_{hf}) of various components (Fe_3O_4(A), Fe_3O_4(B), α-FeOOH, and amorphous Fe_3O_4) decreased after the adsorption of U(VI) in comparison with raw magnetite. This suggested that the geometry of iron oxide was destructed during the adsorption of U(VI). Hence, it was proved that chemisorption was the main adsorption

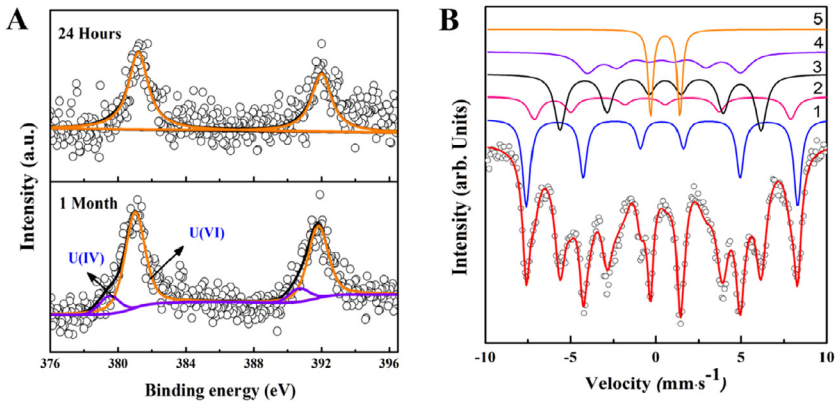

Fig. 7. U4f spectra of U(VI) adsorbed on iron oxides, m/V = 0.6 g L^{-1}, pH = 4.8 ± 0.1, $[UO_2^{2+}]$ = 1.0 × 10^{-5} mol L^{-1}; Mössbauer spectroscopy of magnetite after reaction. 1-Fe_3O_4(A), 2-Fe_3O_4(B), 3-α-FeOOH, 4-amorphous Fe_3O_4, 5-$Fe(OH)_3$, m/V = 0. 6 g L^{-1}, pH = 5.5, $[UO_2^{2+}]$ = 5.0 × 10^{-5} mol L^{-1}.

process of U(VI) on iron oxides, which is consistent with the results above. Li et al. (2017) also demonstrated that the B_{hf} value decreased after chemisorption of Th(IV) on iron oxyhydroxide. More importantly, it is found that the content of magnetic Fe^{3+} in Fe_3O_4(A) increased by 11.67%, while 13.31% of magnetic Fe^{2+}-Fe^{3+} in Fe_3O_4(B) decreased after U(VI) adsorption. The oxidation of structural Fe(II) directly demonstrated the occurrence of the reduction of U(VI), which was in accordance with the results in XPS investigation.

4. Conclusions

Under anaerobic conditions, the adsorption of U(VI) on iron oxides under various physical–chemical conductions was investigated. It was found that pH, HA and temperature played an important role during the process of adsorption. The pseudo-second-order kinetic model could better describe the adsorption kinetics of U(VI) on iron oxides under anaerobic condition. The presence of HA could enhance the U(VI) adsorption under acidic conditions, and reduced the adsorption of U(VI) on iron oxides at near-neutral environment. The formation of $\equiv FeOUO_2^+$ and $\equiv FeOUO^2(OH)^0$ could describe adsorption edge of U(VI) on iron oxides well. Mössbauer spectroscopy and XPS analysis showed that U(VI) was reduced to U(IV) on magnetite after reaction for long time.

CRediT authorship contribution statement

Yun Wang: Methodology, Investigation. **Jingjing Wang:** Software, Validation. **Ping Li:** Conceptualization, Supervision. **Haibo Qin:** Data curation, Writing - original draft. **Jianjun Liang:** Software. **Qiaohui Fan:** Writing - review & editing.

Declaration of competing interest

The authors declare that they have no known competing financial interests or personal relationships that could have appeared to influence the work reported in this paper.

Acknowledgments

Financial supports from National Natural Science Foundation of China (21876172), the "Youth Innovation Promotion Association CAS", Gansu Talent and Intelligence Center for Remediation of Closed and Old Deposits, and the Key Laboratory Project of Gansu Province (1309RTSA041) are acknowledged.

Appendix A. Supplementary data

Supplementary material related to this article can be found online at https://doi.org/10.1016/j.eti.2021.101615.

References

Dodge, C., Francis, A., Gillow, J., Halada, G., Eng, C., Clayton, C., 2002. Association of uranium with iron oxides typically formed on corroding steel surfaces. Environ. Sci. Technol. 36, 3504–3511.

Dong, Z., Zhang, Z., Zhou, R., Dong, Y., Dai, Y., Cao, X., Wang, Y., Liu, Y., 2020. Construction of oxidized millimeter-sized hierarchically porous carbon spheres for U(VI) adsorption. Chem. Eng. J. 386, 123944.

Duro, L., El Aamrani, S., Rovira, M., De Pablo, J., Bruno, J., 2008. Study of the interaction between U(VI) and the anoxic corrosion products of carbon steel. Appl. Geochem. 23, 1094–1100.

Eggleton, R.A., Fitzpatrick, R.W., 1988. New data and a revised structural model for ferrihydrite. Clays Clay Miner. 36, 111–124.

El Aamrani, S., Giménez, J., Rovira, M., Seco, F., Grivé, M., Bruno, J., Duro, L., De Pablo, J., 2007. A spectroscopic study of uranium(VI) interaction with magnetite. Appl. Surf. Sci. 253, 8794–8797.

El Hajj, H., Abdelouas, A., El Mendili, Y., Karakurt, G., Grambow, B., Martin, C., 2013. Corrosion of carbon steel under sequential aerobic–anaerobic environmental conditions. Corros. Sci. 76, 432–440.

Ewing, R.C., 2015. Long-term storage of spent nuclear fuel. Nat. Mater. 14, 252–257.

Fan, F.L., Qin, Z., Bai, J., Rong, W.D., Fan, F.Y., Tian, W., Wu, X.L., Wang, Y., Zhao, L., 2012. Rapid removal of uranium from aqueous solutions using magnetic Fe_3O_4@SiO_2 composite particles. J. Environ. Radioact. 106, 40–46.

Fan, Q.H., Wu, W., Song, X., Xu, J., Hu, J., Niu, Z., 2008. Effect of humic acid, fulvic acid, pH and temperature on the sorption-desorption of Th(IV) on attapulgite. Radiochim. Acta 96, 159–165.

Freundlich, H., 1906. Over the adsorption in solution. J. Phys. Chem. 57, 1100–1107.

Gao, L., Yang, Z., Shi, K., Wang, X., Guo, Z., Wu, W., 2010. U(VI) sorption on kaolinite: effects of pH, U(VI) concentration and oxyanions. J. Radioanal. Nucl. Chem. 284, 519–526.

Grambow, B., Smailos, E., Geckeis, H., Müller, R., Hentschel, H., 1996. Sorption and reduction of uranium(VI) on iron corrosion products under reducing saline conditions. Radiochim. Acta 74, 149–154.

Hattori, T., Saito, T., Ishida, K., Scheinost, A.C., Tsuneda, T., Nagasaki, S., Tanaka, S., 2009. The structure of monomeric and dimeric uranyl adsorption complexes on gibbsite: A combined DFT and EXAFS study. Geochim. Cosmochim. Acta 73, 5975–5988.

Ho, Y.S., McKay, G., 2000. The kinetics of sorption of divalent metal ions onto sphagnum moss peat. Water Res. 34, 735–742.

Janaun, J., Ellis, N., 2011. Role of silica template in the preparation of sulfonated mesoporous carbon catalysts. Appl. Catal. A 394, 25–31.

Langmuir, I., 1918. The adsorption of gases on plane surfaces of glass, mica and platinum. J. Am. Chem. Soc. 40, 1361–1403.

Li, P., Liu, Z., Ma, F., Shi, Q., Guo, Z., Wu, W., 2015. Effects of pH, ionic strength and humic acid on the sorption of neptunium(V) to Na-bentonite. J. Mol. Liq. 206, 285–292.

Li, P., Ma, X., Li, H., Li, S., Wu, H., Xu, D., Zheng, G., Fan, Q., 2017. Sorption mechanism of Th(IV) at iron oxyhydroxide (IOHO)/water interface: Batch, model and spectroscopic studies. J. Mol. Liq. 241, 478–485.

Li, P., Wang, J., Peng, T., Wang, Y., Liang, J., Pan, D., Fan, Q., 2019. Heterostructure of anatase-rutile aggregates boosting the photoreduction of U(VI). Appl. Surf. Sci. 483, 670–676.

Li, P., Yin, Z., Lin, J., Jin, Q., Du, Y., Fan, Q., Wu, W., 2014. The immobilization of U(VI) on iron oxyhydroxides under various physicochemical conditions. Environ. Sci.: Processes Impacts 16, 2278–2287.

Liu, X., Xu, X., Sun, J., Alsaedi, A., Hayat, T., Li, J., Wang, X., 2018. Insight into the impact of interaction between attapulgite and graphene oxide on the adsorption of U(VI). Chem. Eng. J. 343, 217–224.

Mei, H., Liu, Y., Tan, X., Feng, J., Ai, Y., Fang, M., 2020. U(VI) adsorption on hematite nanocrystals: Insights into the reactivity of {001} and {012} facets. J. Hazard. Mater. 399, 123028.

Payne, T., Davis, J., Waite, T., 1996. Uranium adsorption on ferrihydrite-effects of phosphate and humic acid. Radiochim. Acta 74, 239–243.

Qian, L., Ma, M., Cheng, D., 2015. Adsorption and desorption of uranium on nano goethite and nano alumina. J. Radioanal. Nucl. Chem. 303, 161–170.

Rossberg, A., Ulrich, K.U., Weiss, S., Tsushima, S., Hiemstra, T., Scheinost, A.C., 2009. Identification of uranyl surface complexes on ferrihydrite: Advanced EXAFS data analysis and CD-MUSIC modeling. Environ. Sci. Technol. 43, 1400–1406.

Schmeide, K., Pompe, S., Bubner, M., Heise, K., Bernhard, G., Nitsche, H., 2000. Uranium(VI) sorption onto phyllite and selected minerals in the presence of humic acid. Radiochim. Acta 88, 723–728.

Sellin, P., Leupin, O.X., 2013. The use of clay as an engineered barrier in radioactive-waste management–a review. Clays Clay Miner. 61, 477–498.

Shoesmith, D., 2006. Assessing the corrosion performance of high-level nuclear waste containers. Corros 62, 703–722.

Smailos, E., Schwarzkopf, W., Kienzler, B., Köster, R., 1991. Corrosion of carbon-steel containers for heat-generating nuclear waste in brine environments relevant for a rock-salt repository. MRS Online Proc. Libr. 257.

Sylwester, E., Hudson, E., Allen, P., 2000. The structure of uranium(VI) sorption complexes on silica, alumina, and montmorillonite. Geochim. Cosmochim. Acta 64, 2431–2438.

Tsouris, C., 2017. Uranium extraction: fuel from seawater. Nat. Energy 2, 1–3.

Wang, J., He, B., Wei, X., Li, P., Liang, J., Qiang, S., Fan, Q., Wu, W., 2019. Sorption of uranyl ions on TiO_2: effects of pH, contact time, ionic strength, temperature and HA. J. Environ. Sci. 75, 115–123.

Wang, Y., Wang, J., Wang, J., Liang, J., Pan, D., Li, P., Fan, Q., 2020. Efficient recovery of uranium from saline lake brine through photocatalytic reduction. J. Mol. Liq. 308, 113007.